An experimental investigation of reverse end bearing of offshore shallow foundations

Divya S. K. MANA, B.Tech, M.Tech
Centre for Offshore Foundation Systems (M053) and ARC Centre of Excellence for
Geotechnical Science and Engineering,
The University of Western Australia
35 Stirling Highway, Crawley, WA – 6009, Australia
Email: 20674905@student.uwa.edu.au

Susan GOURVENEC, B.Eng, PhD (corresponding author)
Centre for Offshore Foundation Systems, (M053) and ARC Centre of Excellence for
Geotechnical Science and Engineering,
The University of Western Australia
35 Stirling Highway, Crawley, WA – 6009, Australia
Tel: +61 8 6488 3995
Fax: +61 8 6488 1044
Email: susan.gourvenec@uwa.edu.au

Mark F. RANDOLPH, M.A., PhD
Centre for Offshore Foundation Systems, (M053) and ARC Centre of Excellence for
Geotechnical Science and Engineering,
The University of Western Australia
35 Stirling Highway, Crawley, WA – 6009, Australia
Email: mark.randolph@uwa.edu.au

ABSTRACT

Shallow skirted foundations can mobilise uplift resistance from end bearing in the short to medium term. However, uncertainty exists over the magnitude of reverse end bearing resistance compared with resistance in compression, and how this might be affected by a gap between the external face of the foundation skirt and the adjacent soil. The study presented in this paper explored the problem through centrifuge model tests, investigating the effect of skirt embedment ratio on (i) the magnitude of reverse end bearing capacity compared to compression capacity (ii) the uplift displacement associated with spontaneous loss of suction during uplift, and (iii) the effect of a vertical gap on the external skirt-soil interface.

The results show that (i) peak uplift capacity equivalent to compression capacity can be mobilised for a fully sealed foundation with an intact skirt-soil interface, (ii) suction required for reverse end bearing can be maintained through considerable foundation displacement, even for low skirt embedment ratio, and (iii) the presence of a vertical gap along the external skirt-soil interface causes abrupt loss of suction beneath the top plate after minimal foundation displacement, with subsequent uplift capacity being markedly reduced.

Keywords: bearing capacity, centrifuge modelling, clays, footings/foundations, offshore engineering, suction.

Words (intro – conclusions inclusive): 7508. Figures: 18. Tables: 1.

INTRODUCTION

Skirted foundations

Skirted foundations comprise a top plate with a peripheral 'skirt'. The skirt penetrates the seabed until the top plate comes into contact with the seabed confining a soil plug within the skirted compartment. Internal skirts may be provided to increase foundation stiffness and effective rigidity of the soil plug (Mana et al. 2013a). Skirted foundations have a wide range of applications in the offshore oil and gas sector, for example to support gravity based structures, steel jacket structures for offshore wind turbines, as anchors for floating structures, and support for a variety of subsea infrastructure such as manifolds, pipeline end terminations and valve protection systems (e.g. Tjelta et al. 1990; Christophersen et al. 1992; Bye et al. 1995; Miller et al. 1996; Watson and Humpheson 2007). Skirted foundations for subsea structures, which are by far their largest application nowadays, generally have relatively low embedment ranging from 5 % to 30 % of the foundation diameter or breadth, while embedment of 20 % to 50 % of the foundation diameter or breadth is typical for gravity bases, jackets or floating structures. A summary of geometry and loading conditions of a range of offshore shallow foundations installed in the field are summarized in Randolph et al. (2005) and Randolph and Gourvenec (2011).

Offshore loading conditions and reverse end bearing

Skirted foundations may be required to resist tension, either through direct uplift (such as when used as part of a tripod support for a fixed structure or through buoyancy of a floating structure) or more commonly because of high overturning moments on a foundation. In the latter case, tensile stresses beneath the foundation will be limited to only part of the full plan area. The present study is restricted to symmetric uplift

loading, although the principles established through the study are also relevant for the case of high moment loading. The objective is to investigate firstly the principle of whether capacities in uplift and compression are similar, and secondly the extent to which a gap down one region of the peripheral skirts compromises the uplift capacity.

When a skirted foundation is subjected to undrained uplift, negative excess pore pressure or suction (relative to the ambient water pressure) is generated between the foundation top plate and the soil plug, which enables a 'reverse' end bearing mechanism to be mobilised (similar to a general shear failure mechanism observed in compression, but in reverse). Reverse end bearing resistance may be of an order of magnitude greater than simple frictional resistance between the skirt and the soil.

Several studies have reported observations of reverse end bearing of shallow foundations for specific embedment ratios under undrained uplift (e.g. Puech et al. 1993; Watson et al. 2000; Watson and Randolph 2006; Acosta-Martinez et al. 2008; Gourvenec et al. 2009; Mana et al. 2012a, b). The potential for improved uplift resistance of skirted foundations due to suction is evident and is acknowledged by current shallow foundation design recommendations (e.g. ISO 2003; API 2011), but the guidelines are general and provide no specific guidance on the effect of factors that may affect the reverse end bearing potential.

Quantitative data on whether or not 'full' reverse end bearing is mobilised is sparse since often tension and compression are not considered in the same study and when they are, consistent findings have not been reported. Some studies (Watson et al. 2000; Mana et al. 2012a, b) reported equal magnitudes of ultimate net undrained bearing capacities in compression and uplift whereas others (Clukey and Morrison 1993; Acosta-Martinez et al. 2008) observed up to 30 % reduction in uplift capacity

compared to compression capacity. Theoretically, the peak uplift and compression capacities should be equal if full reverse end bearing is mobilised. Differences can arise due to partial drainage around the skirt, causing an increase in the compression capacity and decrease in the uplift capacity.

Gapping

Reverse end bearing can only be mobilised while suction is maintained between the top plate and soil plug. The presence of a vertical gap along the skirt-soil interface may jeopardise full reverse end bearing resistance. A gap provides access to free water, potentially to tip level, which will permit more rapid loss of suction at the underside of the top cap. An alternative mechanism is that the presence of free water at tip level may lead to a tension crack opening across the base of the foundation, preventing reverse end bearing being mobilised. However, the extent of the effect of gapping and the potential failure mechanisms that may arise are not well understood or documented.

A gap along the skirt-soil interface may be initiated and propagated by overturning and horizontal loading on the structure due to environmental loading or in-service production processes. Amongst various processes that may lead to gap formation, sustained lateral loading and displacement of a skirted foundation, such as occur in subsea systems due to thermal expansion and contraction of pipelines, are perhaps the most readily imagined. Typical serviceability limits for horizontal displacement are around 0.1 m (Dimmock et al. 2013), which would be sufficient for a gap to form down the side of the skirts on the trailing edge of the foundation.

A gap has greater potential to be formed and remain open the higher the soil strength ratio $s_u/\gamma'z$ (Britto and Kusakabe 1982; Coffman et al. 2004; Supachawarote et al.

2005). Analytical solutions (Britto and Kusakabe 1982) indicate that the minimum strength ratio necessary for the stability of an axisymmetric excavation in soft clay varies from around 0.25 to 0.18 for unsupported excavations with an excavation depth to diameter ratio of 0.1 to 0.5. A gap is unlikely to form in a deposit with strength ratio less than this value, even under significant displacements. Should a gap form, it will close, or 'self-heal', since the soil strength will be insufficient to support the exposed face of the gap. An over consolidated soil profile was adopted in this study with a value of $s_u/\gamma'z$ ranging from 1 to 0.35 for gap depths corresponding to foundation embedment ratios d/D of 0.1 to 0.5, where d is the skirt embedment and D is the foundation diameter. Thus, a gap would be expected to stay open in the foundation tests in this study.

The effect of a gap on uplift resistance of a skirted foundation with embedment ratio d/D = 0.3 in lightly over consolidated kaolin was studied through centrifuge modelling by Acosta-Martinez et al. (2010). Two undrained uplift tests were carried out – one immediately after the generation of a gap and another after a significant waiting period, corresponding to ~ 50 – 70 % of full primary consolidation according to numerical predictions (Gourvenec and Randolph 2010). It is also notable that the centrifuge was ramped down following installation to seal the foundation at 1 g prior to spinning back up for the gap creation, re-consolidation and foundation uplift. The study reported negligible effect of gapping on undrained uplift capacity, when uplift was applied immediately after formation of the gap, but resistance was reduced to 60 % when uplift was applied after an extended period of consolidation.

Summary

The main issues motivating this study, which have not previously been addressed systematically for a range of foundation embedment ratios, are: (i) the potential for full reverse end bearing of shallow skirted foundations to be mobilised; (ii) the magnitude of foundation displacement over which reverse end bearing can be maintained; and (iii) the effect of gapping on reverse end bearing.

SCOPE OF THE PRESENT STUDY

The present study has investigated the undrained uplift and compression resistance of skirted foundations with a range of embedment ratios, $0.1 \leq d/D \leq 0.5$. This range of embedment ratio covers the critical range for shallow skirted foundations most commonly used in practice, particularly in deep water. Centrifuge model test results were used to assess the load-displacement response in undrained uplift and determine if full reverse end bearing could be mobilised. Foundations with an intact skirt-soil interface and with a vertical gap along the external skirt-soil interface were considered.

The study concentrated on vertical uplift to assess the reverse end bearing capacity, although the main principles established are also considered applicable to cases where tensile stresses beneath the foundation arise from overturning moments. Only monotonic loading conditions were investigated, in order to establish a benchmark of uniaxial uplift from which more complex loading conditions may be considered.

In practice, offshore foundations experience a range of load paths including cyclic components of load. Interaction between multi-axial loads and cyclic loading will generally diminish the (vertical) load carrying capacity, but such changes should be considered relative to the benchmark of monotonic uniaxial uplift, as considered in this study.

In the tests undertaken to explore the effect of gapping, the gap was created deliberately by horizontal translation of the foundation. This is consistent with the main focus of the study, which was to assess the effect of gapping, rather than the (varied) loading conditions that might cause gapping.

EXPERIMENTAL SETUP

Drum Centrifuge

All the model tests described here were conducted in the drum centrifuge facility at the University of Western Australia (Stewart et al. 1998) that is equipped with high-speed wireless data acquisition systems (Gaudin et al. 2009). The centrifuge has an outer diameter of 1.2 m, with an annular channel of radial depth 200 mm and height 300 mm. The test acceleration is limited to 300 g. The drum centrifuge has two key parts - the channel and a central tool table. The actuator that controls vertical and radial movement of the model is placed over the central tool table. The channel and the tool table are connected to a Dynaserv motor through two concentric shafts connected through a clutch. This clutch is engaged or released respectively in order to spin the channel and actuator together or independently. With the clutch released, the actuator can be brought to rest while the channel containing the soil sample continues to spin; this facilitates changing and cleaning of foundation models and site investigation tools without stopping the centrifuge. It is also possible to rotate the central tool table, on which the actuator sits, relative to the channel in a load or displacement controlled manner.

Foundation Models

Circular skirted foundations with a single peripheral skirt were fabricated in-house from anodised aluminium. All models had a diameter of 60 mm and the skirt depth was varied to achieve embedment ratios of $d/D = 0.1$, 0.2, 0.3 and 0.5. Skirt wall thickness (t_w) was constant for all models with $t_w/D = 0.008$.

The model diameter was selected to optimise the test layout in the centrifuge while the range of embedment ratio and skirt thickness was selected to represent field conditions. The centrifuge tests were carried out at 200 g giving a prototype diameter $D = 12$ m. Results are presented in terms of the dimensionless quantities, d/D, z/D, V/As_{u0} and kD/s_{um} such that the results are not tied to the specific foundation geometry and soil conditions considered. Figure 1 shows a photograph of all the models used in this study.

The foundations were equipped with local total pressure transducers (TPTs) and pore pressure transducers (PPTs) for monitoring total pressure and the generation and dissipation of excess pore water pressures. Figure 2 shows a schematic of the geometry, notation adopted and placement of local instrumentation on the foundation models. One PPT and two TPTs were provided flush with the underside of the top plate near the centre and periphery along the centreline of the foundation; one PPT was attached at the skirt tip level in a thin cylindrical housing; and two TPTs were provided flush with the outer skirt surface near skirt tip level, diametrically opposite to each other. In order to keep the geometry of the foundation models symmetric, an aluminium cylinder was provided diametrically opposite to the cylindrical housing accommodating the PPT at skirt tip level (shown in grey in Figure 2). The PPT at skirt tip level was used to identify touch-down of the skirts on the soil sample. The TPTs on the skirt face were used to confirm the verticality of the foundation installation and penetration or extraction, and the successful generation and continued openness of

any gap. The transducers on the underside of the top plate were used to identify touchdown of the top plate on the soil surface and to monitor excess pore pressures and total pressures developed during undrained compression and uplift. The transducers were saturated and calibrated in de-aired water inside a pressure chamber, (fixed to the model foundation) prior to all centrifuge tests.

A drainage valve was used to allow egress of water from inside the skirt compartment during installation and completely seal the foundation during loading. The valve works under air pressure, closing when pressure is applied and opening when it is released. In order to check the sealing provided by the valve, initial tests were conducted by immersing the foundation in the surface water with the valve open, then closing it and lifting the foundation above the water surface. If the skirt compartment is completely sealed, it is able to hold water above the free water surface due to the surrounding atmospheric pressure. The water pressure inside the skirt compartment was continuously monitored through the readings from the PPT on the top plate. The foundation was held above the water surface for around an hour to ensure that the sealing was not lost with time.

Soil sample preparation and shear strength characterization

The foundation tests were carried out in a lightly over consolidated kaolin clay. Commercially available kaolin clay powder was used to prepare the soil sample. The properties of this clay are well established (Stewart 1992; Acosta-Martinez and Gourvenec 2006). The clay has a specific gravity, $G_s = 2.6$, liquid limit, LL = 61 %, plastic limit, PL = 27 % and plasticity index, $I_p = 34$.

For preparing the sample, the clay powder was mixed initially with 120 % of water, corresponding to twice the liquid limit, and poured into the centrifuge channel

spinning at 30 g. The clay slurry was allowed to consolidate at 200 g inside the channel and further 'top-ups' of clay were supplied over the following three days to ensure sufficient final depth of clay. After the final 'top-up', the clay sample was allowed to consolidate for four more days at 200 g during which a uniform normally consolidated soil sample was achieved.

Full consolidation of the soil sample was assessed by conducting T-bar tests (Stewart and Randolph 1991, 1994), ensuring a linearly increasing shear strength profile (Figure 3). Once full (primary) consolidation was achieved, the centrifuge was stopped and the top 60 mm of clay was scraped off to achieve a lightly over consolidated (LOC) sample. The newly prepared LOC sample was re-consolidated for a day at 200 g. During sample preparation, the sample was flooded during consolidation stages to prevent the clay surface from drying out.

The miniature T-bar used in the centrifuge comprises a cylindrical cross bar 20 mm long and 5 mm diameter attached at right angles to a long vertical shaft; precise strain gauges located just behind the bar measure the force acting on it during penetration and extraction. It has been general practice to use an average bearing capacity factor or T-bar factor of $N_{T-bar} = 10.5$ for calculating shear strength profiles, based on plasticity solutions (Randolph and Houlsby 1984; Martin and Randolph 2006), but accepting compensating secondary effects of strain rate dependency of shear strength, and partial softening of the clay during passage of the penetrometer (Zhou and Randolph 2009a).

Penetration under undrained conditions is achieved by ensuring that the dimensionless velocity group vD_{T-bar}/c_v is greater than 30 (Finnie and Randolph 1994), where v is the velocity of T-bar penetration, D_{T-bar} is the diameter of the T-bar cylinder and c_v is a

representative coefficient of consolidation of the soil sample. A penetration rate of

1 mm/s was adopted in this study, giving $vD/c_v > 60$, taking a representative value of

the coefficient of consolidation, $c_v = 2.6$ m^2/year (Acosta-Martinez and Gourvenec

2006).

Figure 3 shows the nominal shear strength profile (measured penetration or extraction

resistance (q_{T-bar}) divided by a constant T-bar factor, N_{T-bar}) of the initially prepared

normally consolidated (NC) sample and the 'trimmed' lightly over consolidated (LOC)

sample including cyclic tests, obtained with a constant T-bar factor of 10.5 throughout

the penetration depth. Figure 4 shows the shear strength profile of the LOC soil

sample only, corrected for buoyancy and shallow embedment of the T-bar after the

procedures proposed in White et al. (2010).

The shear strength profile of the LOC sample can be expressed as a linear function of

depth:

[1]
$$s_u = s_{um} + kz$$

where s_{um} is the shear strength at the mudline = 7 kPa, k is the gradient of increase in

shear strength with depth = 1.3 kPa/m and z is the depth below the mudline. Soil

strength heterogeneity can be described by the dimensionless group kD/s_{um}, ranging

from 0 for a uniform shear strength profile to ∞ for a normally consolidated sample,

and is equal to 2.2 here for the 12 m diameter foundation.

Figure 5 shows the over consolidation ratio (OCR) with depth, based on a submerged

unit weight 7 kN/m^3 indicating OCR of 11 at a depth of 10 % of the foundation

diameter and 3 at a depth of 50 % of the foundation diameter (the range of skirt depths

explored).

TEST PROCEDURE

The soil sample was flooded to the maximum depth (i.e. to the top of the channel, giving about 80 mm of standing water) prior to testing to ensure uplift resistance was not limited by cavitation pressure. At the mudline, an ambient water pressure of 160 kPa acted providing the capability for the foundation to take a maximum uplift resistance (load averaged over the foundation area) of more than 260 kPa (160 kPa + atmospheric pressure) before cavitation would occur. In the tests conducted for this study, a maximum tensile resistance of less than 170 kPa was anticipated for the foundation with the highest embedment ratio ($d/D = 0.5$), assuming a bearing capacity factor $N_c = 11$ for $kD/s_{um} = 2$ (Gourvenec and Mana 2011) and shear strength at skirt tip level at installation, $s_{u0} = 14.8$ kPa (see Figure 4).

The foundation model was aligned in the centrifuge with the TPTs on the skirt face positioned in the plane of gap formation (i.e. X-X in Figure 2 set circumferentially in the channel).

All the model tests were carried out at 200 g at a displacement rate of 0.1 mm/s to achieve an undrained soil response. Both installation and loading were carried out at the same rate. The dimensionless group vD/c_v is then about 70, ensuring undrained conditions with respect to the whole foundation, but accepting some local consolidation or swelling around the skirt tips since $vt_w/c_v \sim 0.6$.

The model was installed until the base of the foundation top plate completely touched the soil surface, confirmed by the load cell, and top plate TPT and PPT readings. The drainage valve was kept open during installation and closed immediately after installation, followed by a waiting period of 5 minutes. The waiting period was equivalent to a prototype consolidation time of 138 days or $T = c_v t/D^2 \sim 0.007$,

corresponding to less than 10 % of full primary consolidation according to numerical

solutions (Gourvenec and Randolph 2010). The waiting period was somewhat

arbitrary, selected such that all foundation tests started from a similar (albeit unknown)

state of effective stress. After the waiting period, the foundation was subjected to

displacement-controlled compression or uplift. For the tests with a gap at the skirt-soil

interface, the gap was generated immediately after closing the drainage valve

following installation. The gap was generated by rotating the actuator through an

angle of 0.5 degrees such that the foundation was displaced from its installed position,

creating a maximum displacement $u/D = 0.067$ (4 mm model scale) at the soil surface.

The process of gap generation took around a second. As for tests with an intact skirt-

soil interface, a period of five minutes elapsed before loading.

RESULTS

Measured and net resistance

Load cell measurements were used to calculate foundation resistance during

installation, compression and uplift. The load cell readings were zeroed at the point

where the skirt tip touched the clay surface. Measured resistance (q_m) was taken as the

measured force divided by the cross-sectional area of the foundation. Net resistance

(q_{net}) was calculated by applying a correction to account for the difference between

the submerged plug weight and the overburden pressure (Tani and Craig 1995):

$$[2] \qquad q_{net} = q_m - \sigma'_v + \left(\frac{W'_{soilplug}}{A_{soilplug}} \right)$$

where σ'_v is the vertical overburden pressure at the skirt tip level, $W'_{soilplug}$ is the

submerged weight of the soil plug inside the skirt compartment and $A_{soilplug}$ is the base

area of the foundation. The correction is minimal during installation but becomes more significant with foundation compression and uplift (while suction is maintained).

Installation resistance

Figure 6 shows the measured installation resistance (q_m) for all the tests. Reasonable repeatability is observed among the different foundations. The sudden increase in resistance occurred when the foundation top plate touched the soil, indicating full installation.

The resistance during installation of a skirted foundation comprises end bearing resistance of the skirt and frictional resistance between skirt wall and soil. It may be calculated as:

[3]
$$Q_i = \left(N_{c0,tip}s_{u0} + \gamma'z\right)A_{tip} + \alpha s_{u,av}A_s$$

where: $N_{c0,tip}$ is the bearing capacity factor for tip resistance; s_{u0} is the shear strength at skirt tip level; A_{tip} is the tip cross-sectional area of the foundation in soil (including instrumentation housing etc); α is the interface friction factor; $s_{u,av}$ is the arithmetic mean of shear strength along the skirt embedment length; and A_s is the sum of the internal and external surface area of the embedded portion of the skirt. The following sections describe the method used to calculate $N_{c0,tip}$ and α using small strain finite element analysis and T-bar penetrometer tests.

Determination of $N_{c0,tip}$

It is common practice to assume a bearing capacity factor of $N_{c0,tip} = 7.5$ for tip bearing of a skirted foundation, equivalent to the bearing capacity factor for a buried strip foundation in uniform clay (Skempton 1951). A range of N_c from 7.5 to 11 for higher embedment ratio suction caissons was noted by Andersen et al. (2005).

Small strain finite element (SSFE) analyses were performed using Abaqus (Dassault Systèmes 2010) to explicitly derive the undrained bearing capacity factors for a thin axisymmetric hollow cylinder penetrating vertically into soil, with the same dimensions as the foundation modelled in the centrifuge. A frictionless interface was assumed on the inside and outside of the shaft so as not to contribute to the measured resistance. The shear strength profile given in Equation 1 was assigned to the soil, with Young's modulus, $E_u = 500s_u$, and Poisson's ratio (ν) = 0.499, to represent undrained conditions.

Figure 7 shows the tip bearing capacity factors calculated from a number of SSFE simulations at different depths in the soil. The bearing capacity factors were calculated according to Equation 3, with Q_i the computed load at penetration, z, and α taken as zero. The tip bearing capacity factor is seen to vary from close to 5.4 at the surface to 11.5 by a depth of z/D = 0.5. The variation of tip bearing capacity factors with depth can be expressed by:

[4]
$$N_{c0,tip} = 5.4\left(1 + \left(\frac{5z}{D}\right)^{p}\right)$$

where p = 0.255 for z/D $\leq$ 0.2 and 0.120 for z/D $\geq$ 0.2.

Determination of α

The variation of $N_{c0,tip}$ discussed above was used to back-analyse the installation resistance from the model tests using Equation 3, in order to evaluate the friction ratio, α. A best fit was achieved with α = 0.3, similar to that observed by Gourvenec et al. (2009) but lower than that reported by Chen and Randolph (2007) (= 0.41 for LOC clays). Installation resistance predicted using Equation 3 with α = 0.3, based on

16

updated $N_{c0,tip}$ values from Equation 4, divided by the base cross-sectional area of the

foundation ($A = \pi D^2/4$) is shown in Figure 6.

The interface friction factor, α, represents the proportion of the undrained shear

strength of the surrounding soil sample that acts as the limiting friction along the skirt

soil interface. The interface friction factor is commonly taken as equal to the

reciprocal of the sensitivity of the soil (Andersen et al. 2005), which can be measured

in the centrifuge from cyclic T-bar tests. Figure 8 shows the resistance measured

during each cycle of penetration and extraction of the T-bar ($q_{u,i}$) normalised by the

initial penetration resistance through intact soil ($q_{u,i=0.25}$) at the mid depth of the cycles.

The first penetration of the T-bar was counted as cycle, i = 0.25, first extraction as

0.75 and subsequent penetrations and extractions as cycles 1.25, 1.75, 2.25, 2.75 and

so on (Zhou and Randolph 2009b). Einav and Randolph (2005) expressed the ratio of

penetration resistance after 'i' cycles to the initial resistance, as

[5]
$$\Delta(i) = \Delta_{rem} + \left(1 - \Delta_{rem}\right)e^{-3(i-0.25)/N_{95}}$$

where Δ_{rem} is the ratio of fully remoulded penetration or extraction resistance to the

initial penetration resistance (taken here as an estimate for α) and N_{95} is the number of

cycles required to achieve 95 % of the degradation. Best fit with the T-bar test results

from the centrifuge was achieved with values of Δ_{rem} (an estimate for α) = 0.39 and

N_{95} = 1.7. The value of interface friction factor, α, back calculated from the measured

installation data (= 0.3, derived from Equation 3) is lower than that estimated from the

cyclic T-bar data. This arises from two factors. The first is that the sensitivity of the

soil itself is greater than the ratio of initial to post-cyclic T-bar resistance, since the

T-bar factor increases during remoulding (Zhou and Randolph 2009b). The second

aspect concerns the differences in shearing modes for the two events, with localised

planar shearing adjacent to the skirts during penetration, compared with diffuse

remoulding of the soil in the zone around the T-bar during cyclic penetration and extraction.

Undrained compression and uplift resistance: Intact skirt-soil interface

Figure 9 illustrates the measured and net undrained, compression and uplift resistance for the foundation with embedment ratio, $d/D = 0.3$, with an intact skirt-soil interface. The results are compared with the upper and lower bound solutions for rough circular skirted foundations in soil with $kD/s_{um} = 2$ as a validation (Martin 2001). The bound stresses are calculated by multiplying the bearing capacity factors by the in situ shear strength at skirt tip level, updated for foundation position from the profile given in Figure 4. It can be seen that the net bearing resistance in compression lies in between the upper and lower bounds and is parallel to the bound lines with increasing penetration.

It can also be noticed that the peak uplift resistance lies between the upper and lower bounds. The theoretical prediction is higher than the actual resistance at larger displacements since the foundation embedment reduces with increasing uplift; this is not taken into account in the bound calculations. In the centrifuge, the resistance is also affected by continuous remoulding of the soil during increased uplift displacement.

Undrained normalised bearing resistance was calculated for each foundation in compression and uplift from the net bearing resistance according to

$$[6] \qquad\qquad N_{c0} = \frac{q_{net}}{s_{u0}}$$

where s_{u0} is the in situ shear strength at the skirt tip level (i.e. as shown in Figure 4).

Figure 10 shows two different representations of normalised bearing capacity against normalised skirt embedment: (a) using a single value of in situ shear strength, taken at the initial installation depth (different for each foundation depending on the skirt

embedment depth), represented by the black lines; and (b) updating the shear strength at skirt tip level with changing elevation of the foundation, during either compression or uplift, presented in the figure using grey lines. Updating the undrained shear strength with elevation leads to a steady-state value of bearing capacity factor in compression. The steady state bearing capacity factors in compression and the peak bearing capacity factors in uplift for each of the foundations are shown in Figure 11 along with lower and upper bound solutions (after Martin 2001). It can be seen that the experimentally derived bearing capacity factors fall between the theoretical bound solutions, and that the peak undrained uplift capacity is approximately equal to the steady-state undrained compression capacity (with a maximum difference of 2 %) indicating that near-full reverse end bearing was achieved in the centrifuge tests when the foundation was fully sealed and an intact skirt-soil interface was maintained. The bearing capacity factors presented in Figure 11 are summarised in Table 1.

Effect of installation depth on uplift response

The importance of installation of the foundations to a common stress level in each test is illustrated in Figure 12, which shows the foundation installation and pullout resistance from three different tests on the same foundation (d/D = 0.2) installed to different loads (and thus penetrations). Maximum peak uplift capacity is mobilised when the foundation is just installed (A in Figure 12). Peak uplift capacity is reduced when the foundations are 'over loaded' during installation (B and C in Figure 12).

The same procedure was adopted for installing and loading all the foundations, which is evident from the overlying resistance profiles during installation of the foundations. After installation, an equal waiting period of 5 minutes (T ~ 0.007) was allowed in all the tests. It can be observed that when the foundation was over-penetrated through a distance of 0.6 % and 1.3 % of the foundation diameter (marked B & C respectively),

the peak value of uplift resistance reduced by around 7 % and 18 % respectively of the peak uplift resistance for the 'just installed' case (marked A). However, suction is maintained inside the skirt compartment over larger uplift displacement for the over-loaded cases. Suction was maintained for displacements equivalent to 0.054D, 0.092D and 0.112D for cases A, B and C respectively.

The lower peak uplift resistance with higher installation load and penetration is attributed to some remoulding caused by over-penetration, which does not occur in virgin uplift. An extreme case of this was discussed by Watson et al. (2000), where over-penetration by d/2 led to a very soft response in uplift, with significant reduction in uplift resistance. The processes involved are complex, and can only be inferred from the centrifuge data, but the phenomenon may partly explain the lower uplift capacity observed in some other experimental studies (e.g. Clukey and Morrison 1993; Acosta-Martinez et al. 2008).

The over-penetration noted in Figure 12 is a feature of the jacked installation procedure adopted in the centrifuge tests. In the field, skirted foundations are more likely to be installed by active suction, such that over-penetration would not occur. This implies that in the field the more brittle uplift response would be observed, involving higher peak uplift resistance but maintained over relatively smaller uplift displacement.

Detailed analysis of uplift response

Figure 10 indicates similar pre-yield load-displacement response in uplift, irrespective of initial foundation embedment ratio. Failure is brittle at lower embedment ratios, becoming more ductile with increasing embedment ratio. Figure 10 shows peak uplift resistance is mobilised at an uplift displacement ~ 0.02 – 0.05D, increasing with increasing embedment ratio. This corresponds to ~ 0.2d of the skirt depth for the

foundation with d/D = 0.1 to 0.1d for the foundation with d/D = 0.5. Uplift resistance diminishes following mobilisation of peak capacity due to reducing embedment ratio and reducing shear strength in the shallower soil as the foundation displaces upwards. Figure 13 shows the full load-displacement response of each of the uplift tests and indicates the uplift foundation displacement at which suction was abruptly lost. The critical uplift displacement ranged from 0.36d – 0.52d, corresponding to 0.04D - 0.25D. The relative displacement over which suction could be maintained depended largely on the initial installation load (i.e. penetration) and the subsequent brittleness of the load-displacement response, as was also shown in Figure 12.

After losing suction, either (i) the foundation moves upwards holding the soil plug inside the skirt compartment or (ii) the foundation pulls out of the soil without the soil plug. In the first case, the uplift resistance is equal to the submerged weight of the soil plug and external friction along the skirt; in the second case, it is due to the combined internal and external friction along the skirt, and a small contribution from skirt tip resistance.

In order to determine the frictional resistance during pullout of the foundation without the soil plug, a model test was conducted on a selected foundation embedment ratio (d/D = 0.2) with the skirt compartment vented (i.e. unsealed). The same procedure as for the other tests was adopted for the vented test, except that the drainage valve was not closed after the waiting period. Figure 14 shows the installation and extraction resistance for the vented foundation test, expressed as the net load divided by the full cross-sectional area of the foundation. The corresponding installation resistance predicted using Equation 3, assuming $\alpha = 0.3$, is also shown in the figure.

The frictional resistance during extraction, $Q_{e,f}$ can be calculated in a similar manner as

[7] $$Q_{e,f} = \alpha s_{u,av} A_s$$

where A_s is the total internal and external skirt area. The resulting value of interface

friction factor α during extraction is back calculated as $\alpha = 0.6$, double the value

during installation. The increase in α arises from the waiting period following

installation, during which consolidation results in increased effective stresses along

the skirt wall.

The uplift resistance when the soil plug in the skirt compartment is pulled out with the

foundation, $Q_{e,p}$ can be calculated as the sum of soil plug weight and friction between

the outer skirt wall and soil given by,

[8] $$Q_{e,p} = \gamma' d A_i + 0.5 \alpha s_{u,av} A_s$$

where A_i is the internal cross sectional area of the skirt. The resistances calculated

using equations 7 and 8 normalised by the skirt base area A, assuming $\gamma' = 7$ kN/m^3

and $\alpha = 0.6$, are also plotted in Figure 13. The resistance measured in the centrifuge

tests after suction was lost lies in between the resistance due to skirt friction alone and

resistance due to plug weight and skirt friction for each foundation embedment ratio.

It can also be noticed that for the deepest foundation embedment ratio (d/D = 0.5), the

measured resistance after losing suction is parallel to the resistance calculated using

Equation 8, whereas the resistance decreases with displacement for foundations with

lower embedment ratio. This indicates that the foundation with d/D = 0.5 had

sufficient internal skirt friction to hold the soil plug.

Undrained uplift resistance: Effect of gapping at the skirt-soil interface

Figure 15 compares the load-displacement response of the foundations with a sealed

top cap, and either with an intact skirt-soil interface or with a vertical gap created

between the external face of the skirt and the soil. Data are shown for foundations

with embedment ratios d/D = 0.1, 0.2 and 0.3. Unfortunately no data was obtained for

the gapped test with embedment ratio of $d/D = 0.5$ due to failure of the data acquisition during the test and insufficient sites to repeat the test.

The most notable effect of a gap along the skirt-soil interface is the sudden loss of uplift resistance at relatively small uplift displacement compared with the response of the foundation with an intact skirt-soil interface, particularly for the cases of $d/D = 0.1$ and 0.3. It is considered likely that the gap did not remain open in the test with $d/D = 0.2$, as is discussed in more detail later.

The point of failure with the gapped interface varied between the three tests; for the foundation with $d/D = 0.1$ peak uplift resistance is lower in the presence of a gap and loss of uplift resistance is observed at a normalised uplift displacement $w/D = 0.9$ %, compared with 3.6 % with an intact skirt-soil interface. For the foundation with $d/D = 0.2$, peak uplift resistance is again lower in the presence of a gap but loss of uplift resistance is observed at a larger proportion of normalised uplift displacement $w/D = 5.2$ % compared with 9.2 % with an intact skirt-soil interface. For the foundation with $d/D = 0.3$ a higher peak uplift resistance is mobilised in the presence of a gap, although and loss of uplift resistance is observed at minimal uplift displacement $w/D = 1.4$ %, compared with 12 % with an intact skirt-soil interface. The higher load resistance is likely to be due to the increased resistance offered by the compressed soil on the passive side of the foundation resulting from the method of gap formation in the centrifuge.

The effect of gapping on uplift response is less pronounced for the foundation with $d/D = 0.2$, which is due to partial closing of the gap before uplift was applied. This is evident from the readings from TPTs set on the skirt wall near skirt tip at diametrically opposite locations as shown in Figure 16. The figure shows readings from the TPTs on a foundation with embedment ratios (a) $d/D = 0.2$ and (b) $d/D = 0.3$

during the gap tests. TPT3 and TPT4 were located on the active and passive sides of the foundation respectively. The initial portion shows the total pressure on the skirt wall during installation. After that, the gap was generated, indicated by sharply increasing reading of TPT4 and decreasing reading of TPT3. On comparing plots (a) and (b), it can be noticed that in (a) for d/D = 0.2 the readings from TPT4 dropped soon after the gap generation indicating that the foundation moved back towards the installation position, in contrast to the response in (b) for d/D = 0.3. The readings from TPT3 in Figure 16a are stable throughout the waiting period after gap generation, showing that the foundation did not come back fully to its initial position and the gap did not close completely.

The loss of uplift resistance indicated in Figure 15 is reflected in the loss of suction measured by the PPT underneath the top plate. Figure 17 shows the PPT readings from the intact and gapped tests on foundations with d/D = 0.1, 0.2 and 0.3. Comparing the resistance curves in Figure 15 with the pore pressure response in Figure 17, it is clear that the abrupt reduction in uplift capacity coincides with the loss of suction between the top plate and the soil. After losing suction, the pore pressure beneath the top plate falls to around zero in all the tests except for the case of gapped test with d/D = 0.3. It is also noted that, while the ultimate uplift resistance of the foundation with d/D = 0.3 is higher in the presence of a gap than that for the intact case (Figure 15), the maximum negative pore pressure generated in the gap test is lower compared to the intact case (Figure 17).

The degree of conservatism by relying only on frictional skirt-soil resistance is illustrated by comparison of the measured uplift resistance of a vented foundation with the reverse end bearing resistance of the same foundation, d/D = 0.2 (shown in

Figure 14), indicating that frictional resistance may provide less than 10 % of the peak uplift capacity of reverse end bearing.

In summary, the most significant effect of a gap is the loss of suction and hence reduction in uplift resistance at minimal foundation displacement. The magnitude of peak uplift resistance for foundations with a gap is variable, but always above 85 % of the measured peak with an intact skirt-soil interface. While it may be conservative to overlook reverse end bearing capacity in design if suction can be relied on, the consequence of a gap forming along the skirt-soil interface is potentially catastrophic if not mitigated against. Mitigation measures might include provision of internal skirts to compartmentalise the soil plug, so that loss of suction would be limited to a single compartment or group of compartments rather than across the entire foundation footprint. A flexible mat might be provided around the periphery of the foundation to act as a sacrificial pseudo compartment, although the technology for so-called 'gap arrestors' has yet to be established in the field (Mana et al. 2013b). It should also be borne in mind that very soft, normally consolidated clays may not be prone to gapping, so that reverse end bearing response corresponding to an intact skirt-soil interface can be relied on.

Mechanisms of failure

Mechanisms governing failure of skirted foundations in undrained uplift, with either an intact skirt-soil interface or with a vertical gap along the interface between the external skirt and the soil, have not previously been clarified. Hypotheses for mechanisms of failure for these cases are put forward based on the results of the tests presented here.

Intact skirt-soil interface

As the foundation is displaced upwards under undrained conditions, the soil adjacent to the foundation will be dragged down, to maintain constant volume conditions. As a result, the uplift displacement for complete loss of contact along the external skirt will be less than the skirt length, as illustrated schematically in Figure 18a. This proposed failure mechanism is supported by PIV results of 'half-foundation' tests presented by Mana et al. (2012a). Those tests showed clear downward movement of soil adjacent to the foundation during undrained uplift of circular skirted foundations with embedment ratios d/D between 0.1 and 0.5, as considered in this study. In the present study, passive suction was lost at a maximum foundation displacement, w, equal to around half the skirt depth, for the deepest embedment ratio considered, d/D = 0.5. This corresponds to 'drag-down', denoted by s, of similar magnitude to the upward displacement, w, i.e. a 'drag-down ratio's/w of unity.

Gapped skirt-soil interface

The same constant volume conditions govern undrained deformation of the soil around a foundation with a gap along the skirt-soil interface, causing the soil around the foundation to be dragged down as the foundation is displaced upwards. However, the presence of a gap and the consequent accessibility of free water at skirt tip level introduce the potential for earlier loss of suction under the top plate. This may occur due to ingress of water (i) up the inside face of the skirt due to 'necking' of the soil plug inside the skirted compartment, or (ii) through development of a horizontal tension crack at skirt tip level, essentially severing the soil plug from the soil beneath. Either case can lead to abrupt loss of suction beneath the top plate – as observed in the tests. The proposed mechanisms of failure for a gapped skirt-soil interface are illustrated schematically in Figure 18b.

CONCLUDING REMARKS

The centrifuge tests reported in this paper investigated the compression and uplift capacity of skirted foundations, with a range of embedment ratios ($0.1 \leq d/D \leq 0.5$), in a lightly over consolidated clay. The tests were conducted under undrained conditions, and the uplift responses were compared for conditions either with an intact skirt-soil interface, or with a pre-formed vertical gap along the external skirt-soil interface. The following conclusions can be drawn from the test results and analysis:

- Peak undrained uplift resistance of a similar magnitude to that mobilised in compression was achieved for a range of embedment ratios (as low as $d/D = 0.1$) if the skirt-soil interface remained intact and the foundation remained fully sealed.

- Peak undrained uplift resistance was mobilised at foundation uplift displacements between 2 % and 5 % of the foundation diameter, increasing with increasing embedment ratio.

- Suction beneath the top cap was maintained for foundation uplift displacement between a third and a half the skirt depth for the range of embedment ratios considered, $0.1 \leq d/D \leq 0.5$, for conditions where the skirt-soil interface was initially intact.

- The presence of a gap had a limited effect on the peak uplift capacity, but led to much earlier (and abrupt) loss of suction beneath the top plate, and consequently a rapid and dramatic reduction in uplift capacity with minimal displacement following mobilisation of the peak load.

- Vented uplift resistance (resulting from loss of sealing of the foundation) represented as little as 10 % of full reverse end bearing capacity.

Mechanisms governing undrained failure of skirted foundations have been proposed for cases of both an intact and gapped skirt-soil interface, based on observations and results from the tests presented here. The main mechanism leading to loss of suction for (initially) intact skirt-soil interfaces involves 'drag-down' of the soil adjacent to the foundation as the foundation displaces upwards; this leads to complete loss of suction for uplift displacements of less than the skirt length.

Improved understanding of the conditions for gap initiation and propagation, in conjunction with methods for mitigating gap propagation, or minimising the effect of a gap should one form, will allow improved confidence in relying on skirted foundation response in uplift. Although only uniaxial uplift was considered here, the results should provide conservative guidance for cases where limited regions of tensile stresses result from high moment loading. Increased confidence in the ability for skirted foundations to sustain suction within the skirt compartment has the potential for significant efficiencies in the design of skirted foundations to resist uplift and overturning moments.

ACKNOWLEDGEMENTS

REFERENCES

Acosta-Martinez, H.E. and Gourvenec, S.M. 2006. One-dimensional consolidation tests on kaolin clay, Report Research Report GEO: 06385, Centre for Offshore Foundations Systems, School of Civil and Resource Engineering, The University of Western Australia.

Acosta-Martinez, H.E., Gourvenec, S.M. and Randolph, M.F. 2008. An experimental investigation of a shallow skirted foundation under compression and tension. Soils and Foundations **48**(2): 247-254.

Acosta-Martinez, H.E., Gourvenec, S.M. and Randolph, M.F. (2010). Effect of gapping on the transient and sustained uplift capacity of a skirted foundation in clay. Soils and Foundations **50**(5): 725–735.

Andersen, K.H., Murff, J.D., Randolph, M.F., Clukey, E.C., Erbrich, C.T., Jostad, H.P., Hansen, B., Aubeny, C., Sharma, P. and Supachawarote, C. 2005. Suction anchors for deepwater applications. *In* Proc. 1st Int. Symp. Frontiers in Offshore Geotechnics (ISFOG), Perth, Australia, 19-21 Sept. 2005. pp. 1-30.

API 2011 Recommended Practice 2GEO: Geotechnical and Foundation Design Considerations, 1st Edition, American Petroleum Institute, Washington.

Britto, A.M. and Kusakabe, O. 1982. Stability of unsupported axisymmetric excavations in soft clay. Géotechnique **32**(3): 261-270.

Bye, A., Erbrich, C., Rognlien, B. and Tjelta, T.I. 1995. Geotechnical design of bucket foundations. *In* Proc. Annual Offshore Technology Conf., Houston, OTC 7793, 1-4 May 1995, pp. 869-883.

Chen, W. and Randolph, M.F. 2007. External radial stress changes and axial capacity for suction caissons in soft clay. Géotechnique **57**(6): 499-511.

Christophersen, H.P., Bysveen, S., and Støve, O.J. 1992. Innovative Foundation Systems Selected for the Snorre Field Development. *In* Proc. 6th International Conference on the Behavior of Offshore Structures (BOSS), London, 7-10 July 1992, pp. 81-94.

Clukey, E. C. and Morrison, M. J. 1993. A centrifuge and analytical study to evaluate suction caissons for TLP applications in the Gulf of Mexico. Geotechnical Special Publication, ASCE, 38: 141-156.

Coffman, R.A., El-Sherbiny, R.M., Rauch, A.F. and Olson, R.E.. 2004. Measured horizontal capacity of suction caissons. *In* Proc. Offshore Tech. Conf., Houston, 3-6 May, OTC 16161.

Dassault Systèmes 2010. Abaqus analysis users' manual, Simulia Corp, Providence, RI, USA.

Dimmock, P., Clukey, E.C., Randolph, M.F., Gaudin, C. and Murff, J.D. (2013). Hybrid subsea foundations for subsea equipment. J. of Geotechnical and Geoenvironmental Engineering, ASCE, in press

Einav, I., and Randolph, M. F. 2005. Combining upper bound and strain path methods for evaluating penetration resistance. Int. J. Numer. Methods Eng. **63**(14): 1991-2016.

Finnie, I.M.S., and Randolph, M.F. 1994. Punch-through and liquefaction induced failure of shallow foundations on calcareous sediments. *In* Proc. Int. Conf. on Behavior of Offshore Structures, BOSS '94, Boston, 4-7 July 1994, pp. 217-230.

Gaudin, C., White, D.J., Boylan, N., Breen, J., Brown, T.A., De Catania, S. and Hortin, P. 2009. A wireless data acquisition system for centrifuge model testing. Measurement Science and Technology **20**(9), Paper No. 095709.

Gourvenec, S. M. and Mana, D. S. K. 2011. Undrained vertical bearing capacity factors for shallow foundations. Géotechnique Letters **1**: 101-108.

Gourvenec, S. and Randolph, M. F. 2010. Consolidation beneath circular skirted foundations. Int. J. Geomech., ASCE **10**(1): 22-29.

Gourvenec, S.M., Acosta-Martinez, H.E. and Randolph, M.F. 2009. Experimental study of uplift resistance of shallow skirted foundations in clay under transient and sustained concentric loading. Géotechnique **59**(6): 525-537.

ISO 2003: Petroleum and natural gas industries - Specific requirements for offshore structures - Part 4: Geotechnical and foundation design considerations, ISO 19901-4, 1st Edition, International Standards Organisation, Geneva.

Martin, C.M. 2001. Vertical bearing capacity of skirted circular foundations on Tresca soil. *In* Proc. 15th Int. Conf. on Soil Mechanics and Geotechnical Engineering, Istanbul, 1, 27-31 Aug. 2001, pp. 743-746.

Martin, C.M. and Randolph, M.F. 2006. Upper-bound analysis of lateral pile capacity in cohesive soil. Géotechnique **56**(2): 141-145.

Mana, D.S.K., Gourvenec, S. and Martin, C.M. 2013a. Critical skirt spacing for shallow foundations under general loading. ASCE Journal of Geotechnical and Geoenvironmental Engineering. doi: 10.1061/(ASCE)GT.1943-5606.0000882 (aop for September issue).

Mana, D.S.K., Gourvenec, S. and Randolph, M.F. 2013b. A novel technique to mitigate the effect of gapping on the uplift capacity of offshore shallow foundations. Géotechnique 10.1680/geot.12.P.173 (aop).

Mana, D.S.K., Gourvenec, S.M., Randolph, M.F and Hossain, M.S. 2012a. Failure mechanisms of skirted foundations in uplift and compression. Int. J. Physical Modelling in Geotechnics (IJPMG), 12(2): 47-62.

Mana, D.S.K., Gourvenec, S.M., Randolph, M.F and Hossain, M.S. 2012b. Effect of gapping on the uplift resistance of a shallow skirted foundation. Proc. 7th Int. Offshore Site Inv. & Geotech. Conf., Society of Underwater Technology, London.

Miller, D. M., Frazer, I., and Brevig, P. 1996. The Heidrun Field – Marine Operations. *In* Proc. Annual Offshore Technology Conf., Houston, 3-6 May 1996, OTC 8101.

Puech, A., Iorio, J.-P., Garnier, J. and Foray, P. 1993. Experimental study of suction effects under mudmat type foundations. *In* Proc. Canadian Conference on Marine Geotechnical Engineering,. St. John's, Newfoundland, 3, pp. 1062-1080.

Randolph, M.F. and Houlsby, G.T. 1984. The limiting pressure on a circular pile loaded laterally in cohesive soil. Géotechnique **34**(4): 613-623.

Randolph, M. F., Cassidy, M. J., Gourvenec, S. and Erbrich, C. 2005. Challenges of offshore geotechnical engineering. 16th Int. Conf. on Soil Mechanics and Geotechnical Engineering, Osaka.

Randolph, M. F. and Gourvenec, S. 2011. Offshore Geotechnical Engineering, Spon Press, Oxon

Skempton, A.W. 1951. The bearing capacity of clays. Building research congress, London, England, 11-20 Sept. 1951, pp. 180-189.

Stewart D.P and Randolph M.F. 1991. A new site investigation tool for the centrifuge. *In* Proc. Int. Conf. on Centrifuge Modelling - Centrifuge 91, Boulder, Colorado, 13-14 June 1991, pp. 531–538.

Stewart D.P. 1992. Lateral loading of piled bridge abutments due to embankment construction. PhD Thesis, The University of Western Australia.

Stewart D.P. and Randolph M.F. 1994. T-bar penetration testing in soft clay. Journal of Geotechnical Engineering Division, ASCE **120**(12): 2230–2235.

Stewart, D.P., Boyle, R.S. and Randolph, M.F. 1998. Experience with a new drum centrifuge. *In* Proc. Int. Conf. on Centrifuge '98, Tokyo, Japan, 23-25 Sept. 1998, pp. 35-40.

Supachawarote C., Randolph M.F. and Gourvenec S. 2005. The effect of crack formation on the inclined pullout capacity of suction caissons. *In* Proc. Int. Association for Computer Methods and Advances in Geomechanics Conf., Turin, Italy: Balkema, 19-24 June 2005, pp. 577–584.

Tani, K. and Craig, W.H. 1995. Bearing capacity of circular foundations on soft clay of strength increasing with depth. Soils and Foundations **35**(4): 21-35.

Tjelta, T.I., Aas, P.M., Hermstad, J. and Andenaes, E. 1990. The skirt piled Gullfaks C platform installation. *In* Proc. Annual Offshore Technology Conf., Houston, 7-10 May 1990, OTC 6473.

Watson P.G., Randolph M.F. and Bransby M.F. 2000. Combined lateral and vertical loading of caisson foundations. *In* Proc. Annual Offshore Technology Conference, Houston, 1-4 May 2000, OTC 12195.

Watson, P.G. and Randolph, M.F. 2006. A centrifuge study into cyclic loading of caisson foundations. *In* Proc. Int. Conf. Physical Modelling in Geotech., Hong Kong, 4-6 Aug. 2006, pp. 693-699.

Watson. P. G., and Humpheson, C. 2007. Foundation design and installation of the Yolla-A platform. *In* Proc. 6th Int. Offshore Site Investigation and Geotechnics Conf. Soc. for Underwater Technology, London, UK, 11-13 Sept 2007, pp. 399-412.

White, D. J., Gaudin, C., Boylan, N. and Zhou, H. 2010. Interpretation of T-bar penetrometer tests at shallow embedment and in very soft soils. Can. Geotech. J. **47**(2): 218-229.

Zhou, H. and Randolph, M.F. 2009a. Resistance of full-flow penetrometers in rate-dependent and strain-softening clay. Géotechnique **59**(2): 79-86.

Zhou, H. and Randolph, M.F. 2009b. Numerical investigations into cycling of full-flow penetrometers in soft clay. Géotechnique **59**(10): 801-812.

Table 1. Summary of undrained bearing capacity factors from centrifuge tests

compared with theoretical solutions by Martin (2001)

| d/D | Bearing capacity factor, N_{c0} | | | Uplift |
| | Compression | | | |
	LB	UB	Centrifuge	Centrifuge
0.1	8.05	9.5	8.35	8.25
0.2	8.5	10.5	9.5	9.3
0.3	8.9	11.05	10.15	10.3
0.5	9.45	12.5	11.2	11.35

FIGURE CAPTIONS

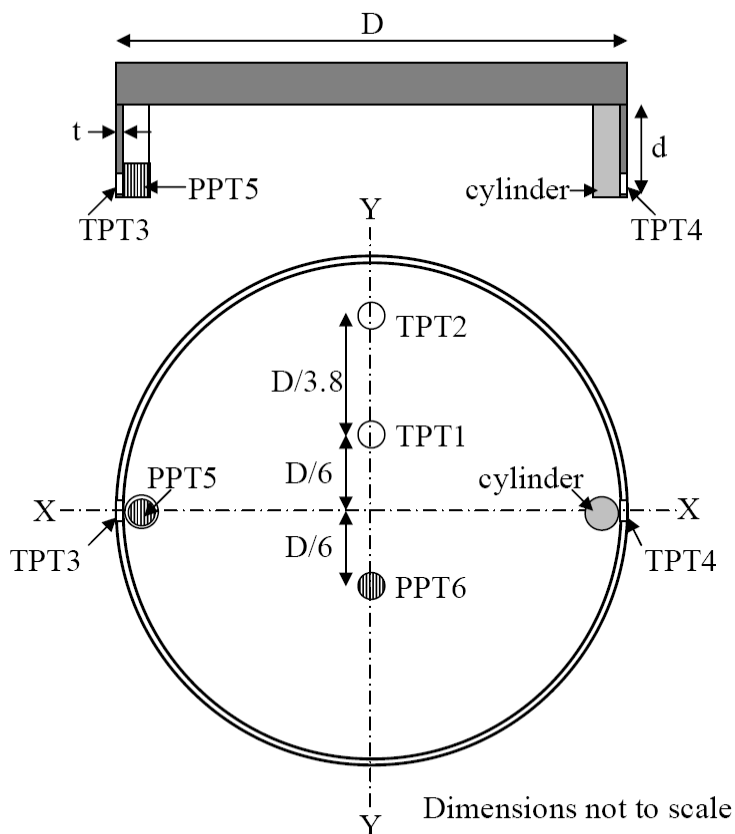Figure 1. Skirted foundation models used for this study

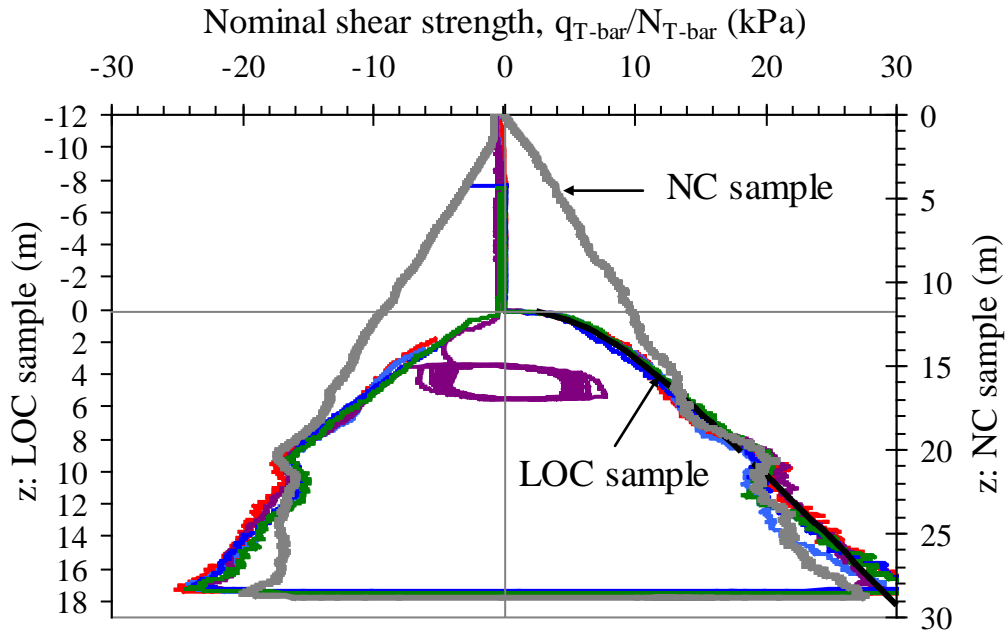Figure 2. Schematic of the sectional elevation and plan of model skirted foundation with instrumentation

Figure 3. Undrained nominal shear strength of NC and LOC soil samples measured from T-bar tests with constant T-bar factor $N_{T-bar} = 10.5$
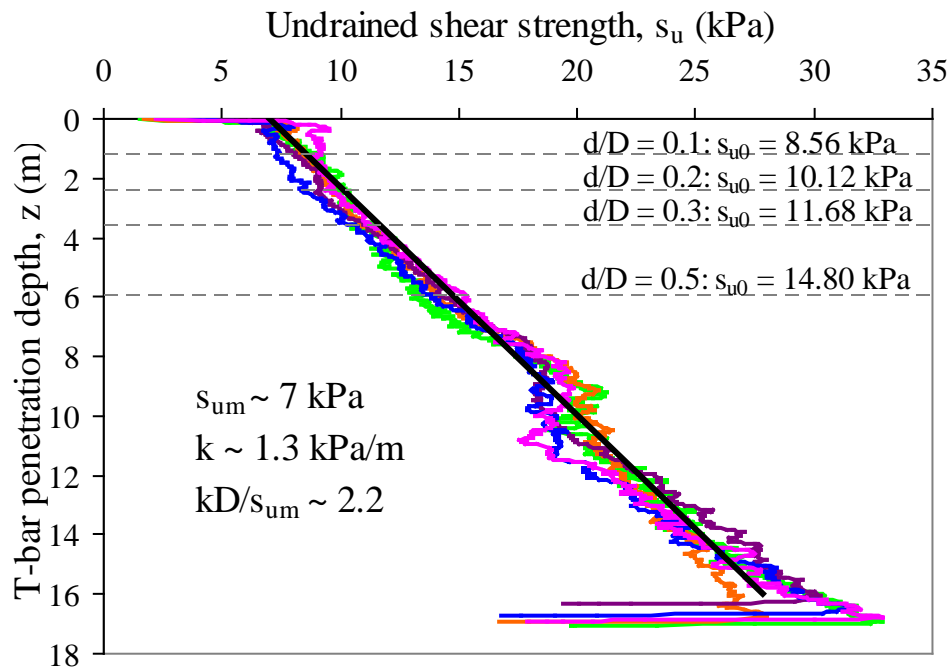
Figure 4. Undrained shear strength profile corrected for soil buoyancy and shallow embedment
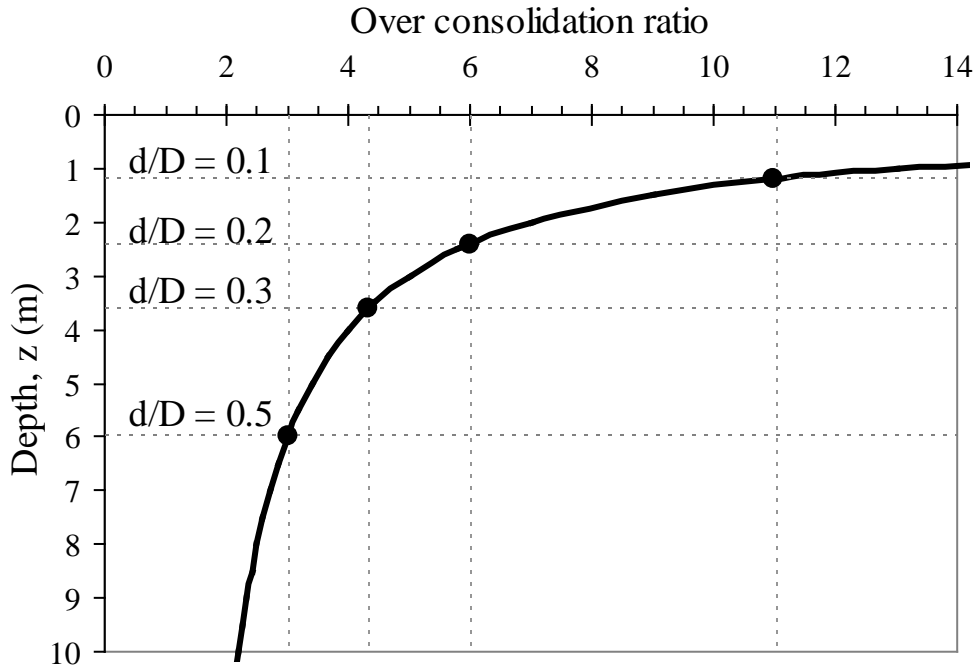
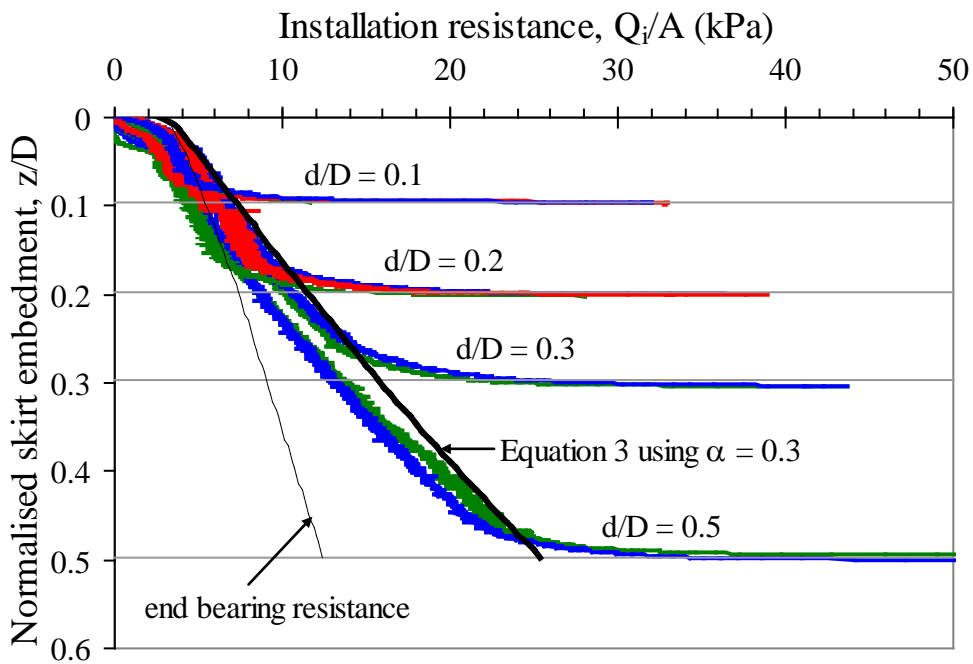Figure 5. Over consolidation ratio of centrifuge sample

Figure 6. Installation resistance from load cell data and back analysis from SSFE analyses
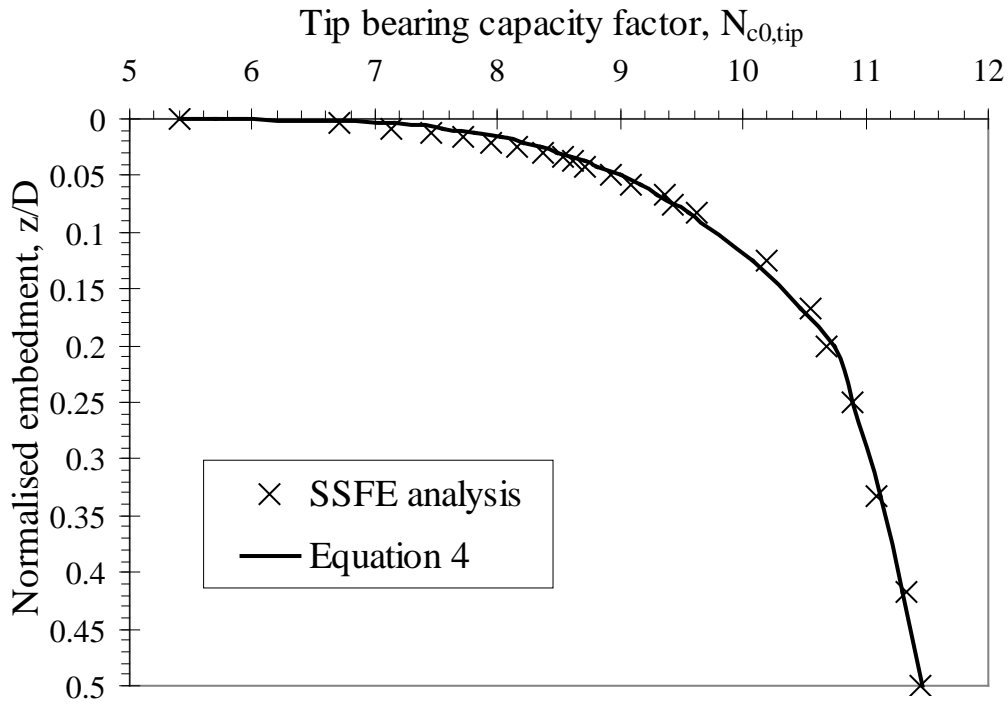
Figure 7. Variation of tip bearing capacity factor with penetration depth; SSFE analyses predictions
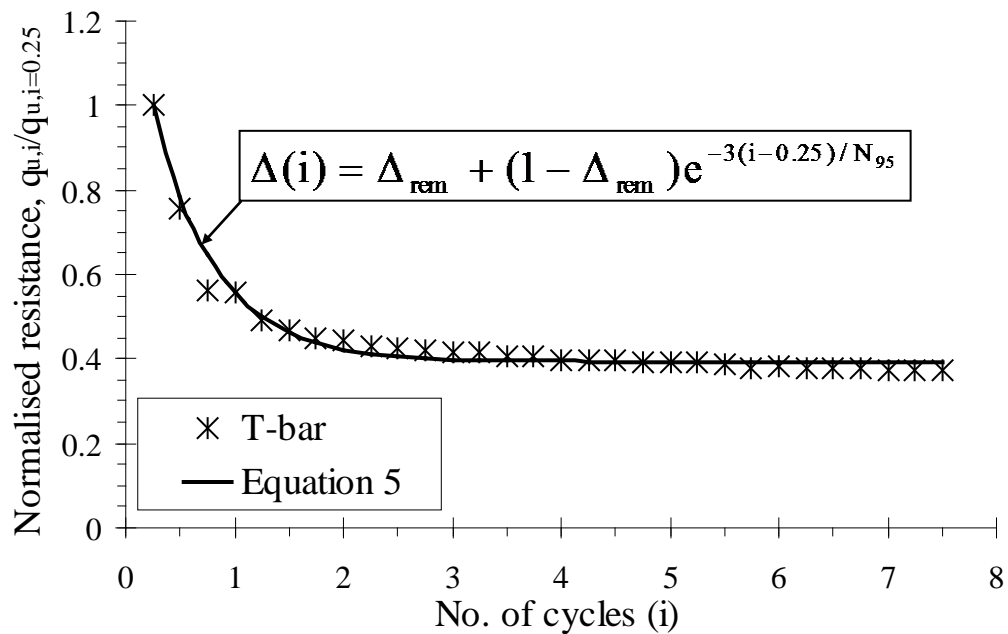
Figure 8. Degradation of penetration and extraction resistance from cyclic T-bar test

Figure 9. Foundation installation and penetration/extraction resistance from load cell data; foundation with d/D = 0.3, intact skirt-soil interface. UB & LB solutions from Martin, 2001.

Figure 10. Undrained normalised bearing response in compression and uplift for foundations with intact skirt-soil interface (black lines correspond to bearing response normalised using single value of shear strength at the initial skirt tip depth and grey lines correspond to bearing response normalised with shear strength updated with embedment depth)

Figure 11. Undrained bearing capacity factors in compression and uplift compared with theoretical solutions

Figure 12. Effect of overloading during installation on the undrained uplift capacity ($d/D = 0.2$)

Figure 13. Uplift load-displacement response of all the foundations studied (w/D is negative to show the upward displacement from installation position)

Figure 14. Installation resistance and vented extraction resistance (following a period of post-installation consolidation)

Figure 15. Effect of gapping on the uplift resistance of foundations with $d/D = 0.1$, $d/D = 0.2$ and $d/D = 0.3$

Figure 16. Readings from the TPTs on skirt wall during the gap tests on (a) $d/D = 0.2$ and $d/D = 0.3$

Figure 17. Readings from PPT underneath the top plate during intact and gap tests

Figure 18. Schematic of proposed failure mechanism of a skirted shallow foundation in undrained uplift with (a) intact skirt-soil interface and (b) gapped skirt-soil interface

Figure 1. Skirted foundation models used for this study

Figure 2. Schematic of the sectional elevation and plan of model skirted foundation with instrumentation

Figure 3. Undrained nominal shear strength of NC and LOC soil samples measured from T-bar tests with constant T-bar factor $N_{T\text{-}bar} = 10.5$

Figure 4. Undrained shear strength profile corrected for soil buoyancy and shallow embedment

Figure 5. Over consolidation ratio of centrifuge sample

Figure 6. Installation resistance from load cell data and back analysis from SSFE analyses

Figure 7. Variation of tip bearing capacity factor with penetration depth; SSFE analyses predictions

The equation shown in the figure:

$$\Delta(i) = \Delta_{rem} + (1 - \Delta_{rem})e^{-3(i-0.25)/N_{95}}$$

Figure 8. Degradation of penetration and extraction resistance from cyclic T-bar test

Figure 9. Foundation installation and penetration/extraction resistance from load cell data; foundation with d/D = 0.3, intact skirt-soil interface. UB & LB solutions from Martin, 2001.

Figure 10. Undrained normalised bearing response in compression and uplift for foundations with intact skirt-soil interface (black lines correspond to bearing response normalised using single value of shear strength at the initial skirt tip depth and grey lines correspond to bearing response normalised with shear strength updated with embedment depth)

Figure 11. Undrained bearing capacity factors in compression and uplift compared with theoretical solutions

Figure 12. Effect of overloading during installation on the undrained uplift capacity (d/D = 0.2)

Figure 13. Uplift load-displacement response of all the foundations studied (w/D is negative to show the upward displacement from installation position)

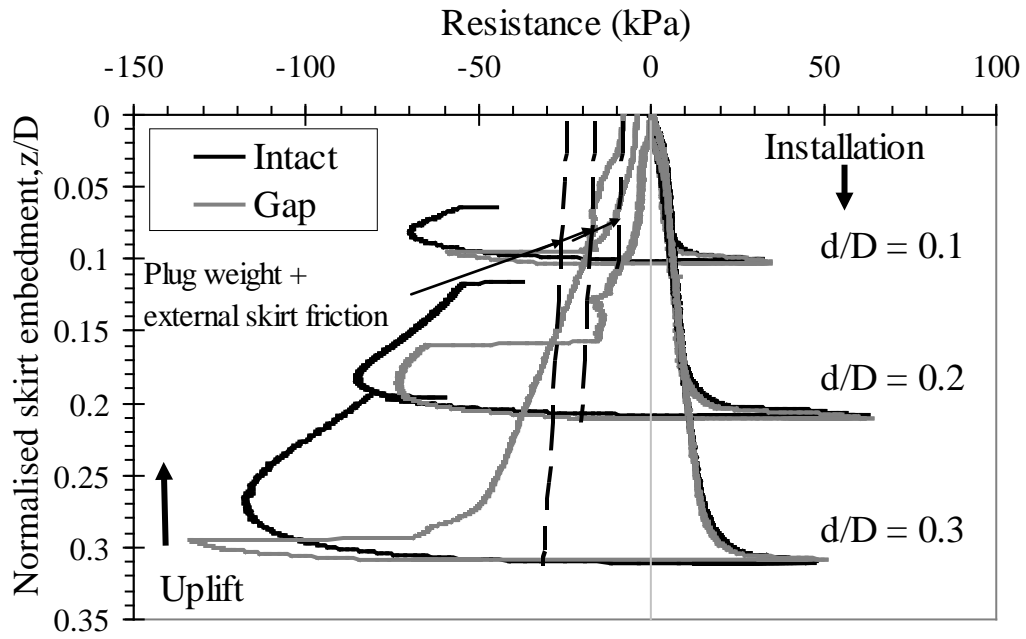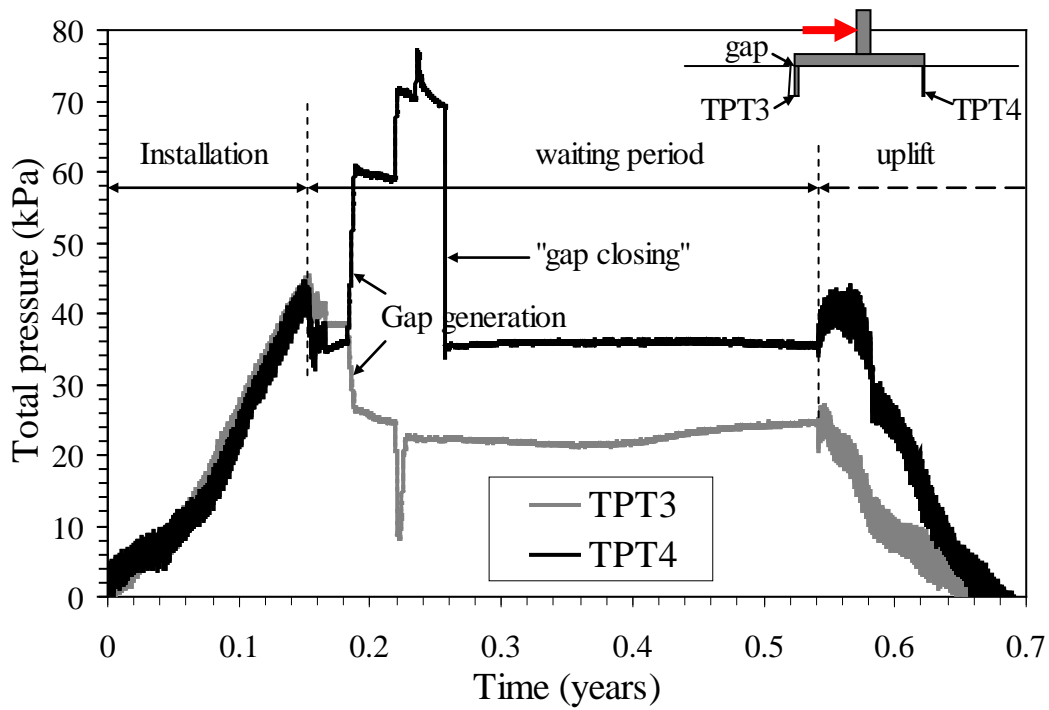**Figure 14. Installation resistance and vented extraction resistance (following a period of post-installation consolidation)**
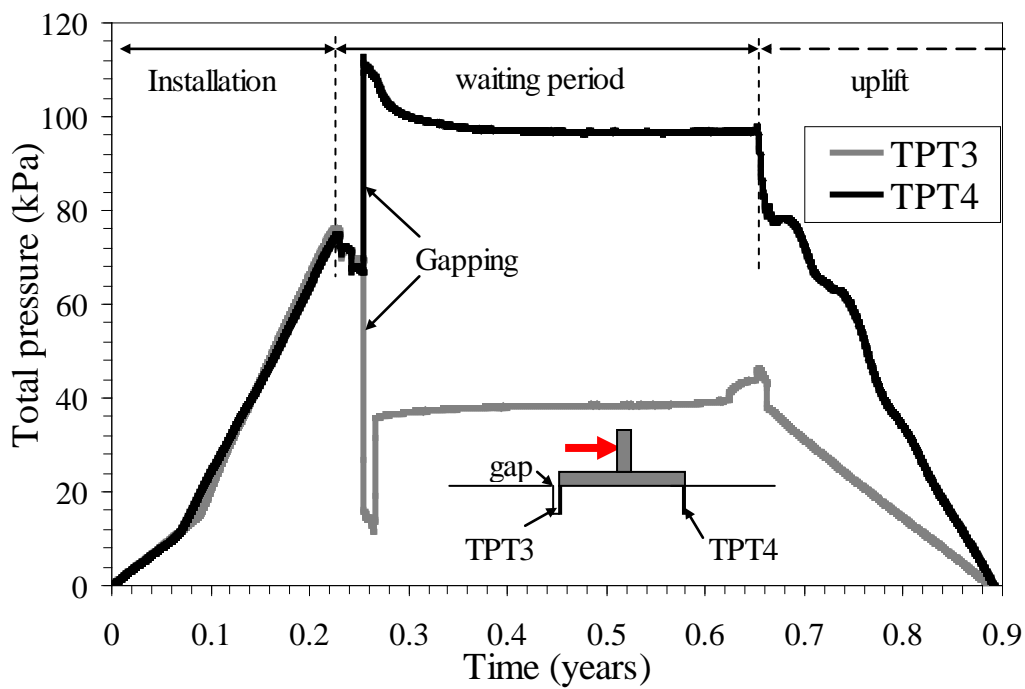
Figure 15. Effect of gapping on the uplift resistance of foundations with d/D = 0.1, d/D = 0.2 and d/D = 0.3

(a)

(b)

Figure 16. Readings from the TPTs on skirt wall during the gap tests on (a) d/D = 0.2 and d/D = 0.3
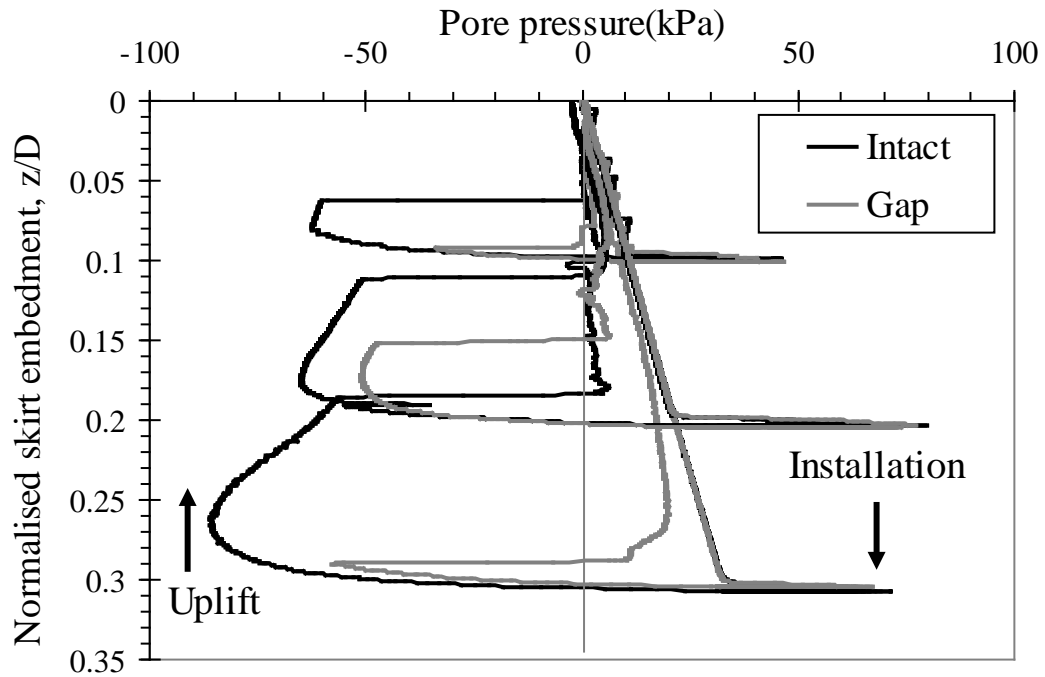
Figure 17. Readings from PPT underneath the top plate during intact and gap tests
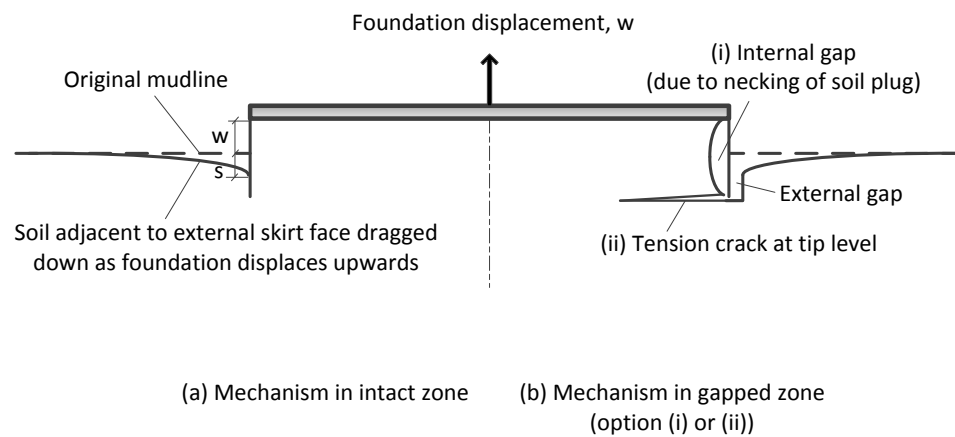

Figure 18. Schematic of proposed failure mechanism of a skirted shallow foundation in undrained uplift with (a) intact skirt-soil interface and (b) gapped skirt-soil interface